JACS
JOURNAL OF THE AMERICAN CHEMICAL SOCIETY
Article
pubs.acs.org/JACS

Why is the Ir(III)-Mediated Amido Transfer Much Faster Than the Rh(III)-Mediated Reaction? A Combined Experimental and Computational Study

Yoonsu Park,[†,‡] Joon Heo,[†] Mu-Hyun Baik,*[,‡,†] and Sukbok Chang*[,‡,†]

[†]Department of Chemistry, Korea Advanced Institute of Science and Technology (KAIST), Daejeon 34141, Republic of Korea
[‡]Center for Catalytic Hydrocarbon Functionalizations, Institute for Basic Science (IBS), Daejeon 34141, Republic of Korea

Supporting Information

ABSTRACT: The mechanism of the Ir(III)- and Rh(III)-mediated C−N coupling reaction, which is the key step for catalytic C−H amidation, was investigated in an integrated experimental and computational study. Novel amidating agents containing a 1,4,2-dioxazole moiety allowed for designing a stoichiometric version of the catalytic C−N coupling reaction and giving access to reaction intermediates that reveal details about each step of the reaction. Both DFT and kinetic studies strongly point to a mechanism where the M(III)-complex engages the amidating agent via oxidative coupling to form a M(V)−imido intermediate, which then undergoes migratory insertion to afford the final C−N coupled product. For the first time, the stoichiometric versions of the Ir- and Rh-mediated amidation reaction were compared systematically to each other. Iridium reacts much faster than rhodium (~1100 times at 6.7 °C) with the oxidative coupling being so fast that the activation of the initial Ir(III)-complex becomes rate-limiting. In the case of Rh, the Rh−imido formation step is rate-limiting. These qualitative differences stem from a unique bonding feature of the dioxazole moiety and the relativistic contraction of the Ir(V), which affords much more favorable energetics for the reaction. For the first time, a full molecular orbital analysis is presented to rationalize and explain the electronic features that govern this behavior.

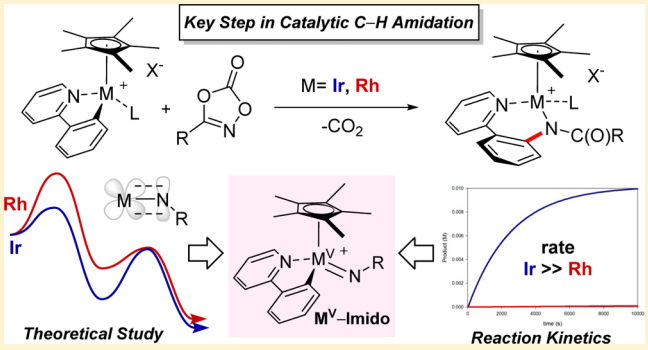

INTRODUCTION

Catalytic amination of C−H bonds is an efficient and direct method for accessing molecular fragments that contain C−N bonds, which play a pivotal role in functional materials, natural products, and pharmaceutical agents.[1] In general, two distinct mechanisms are widely accepted.[2] The first, often referred to as *outer-sphere* C−H amination, is illustrated on the left-hand side in Scheme 1 and assumes that a metal−nitrenoid complex **A** is formed by oxidative coupling from an appropriate precursor, such as iminoiodinane or organic azides.[3] Inter- or intramolecular insertion of the nitrene functionality into the C−H bond may afford the aminated product.[4] Although this relatively simple mechanism is plausible and is accepted widely, recent work provided strong evidence for a more complicated involvement of a high-valent metal−nitrenoid complex in the catalytic process. For example, Che and Gallo reported the characterization of one such intermediate, namely, bis(imido)-ruthenium(VI) porphyrin.[5] In another study, a putative Rh−nitrenoid intermediate was detected using mass spectrometric techniques.[6] Furthermore, an iron(III)−imidyl complex capable of catalyzing C−H bond cleavage was recently reported.[7] These examples illustrate that metal−nitrenoids relevant to catalytic aminations are readily accessible with a variety of transition metals and ligand systems. Yet, their mechanistic roles remain poorly understood, and it is currently impossible to qualitatively predict how an Ir−nitrenoid will behave differently from a Rh−nitrenoid.

The catalytic systems based on the *outer-sphere* pathway are known to work more effectively with benzylic or allylic C(sp^3)−H bonds, whereas unactivated primary or sp^2-

Scheme 1. General Mechanism of Catalytic C−H Amination

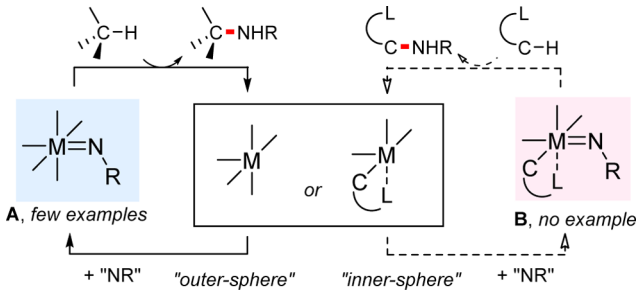

Received: August 7, 2016
Published: October 3, 2016

DOI: 10.1021/jacs.6b08211
J. Am. Chem. Soc. 2016, 138, 14020−14029

hybridized C−H bonds proved difficult to functionalize.[5c,8] A promising strategy to force these strong C−H bonds to react in a selective manner is to utilize a chelating group to direct the C−H bond cleavage, affording a metallacycle, as illustrated on the right-hand side of Scheme 1.[9] The resulting metallacyclic intermediate may react with a nitrogen source to form the C−N bond. Over the past decade, a few catalysts based on late transition metals were discovered and proposed to function following this mechanism.[10] Because both components of the reaction are tightly bound to the metal, this mechanism is referred to as *inner-sphere* C−H amination.

Whereas the *outer-sphere* amination mechanism is reasonably well-established, the *inner-sphere* pathway to C−N coupling remains under debate. Specifically, relevant key intermediates, such as complex **B** in Scheme 1, could not be detected thus far, presumably owing to the highly reactive nature of these putative intermediates.[11] As a result, most of the mechanistic proposals are based on theoretical studies. Previously, Che and Sanford proposed a Pd−nitrenoid complex as a key intermediate for the ligand-directed C−H amination, as shown in Scheme 2a.[12] Ke and Cundari examined such an intermediate by DFT calculations and concluded that a singlet Pd(IV)−imido complex is a plausible intermediate.[12e] We proposed previously that Cp*Rh(V)− and Cp*Ir(V)−nitrenoid complexes are key intermediates during catalytic C−H amination using organic azides, as described in Scheme 2b.[13,14] Several theoretical studies by us[15] and others[16] suggested that the formations of high-valent Cp*M(V)−imido complexes are feasible. Regrettably, direct experimental evidence for the putative metal−nitrenoid complex, such as characterization in a kinetic experiment, spectroscopic detection, or isolation, remained elusive to date. An isolobal Ru(II)-complex was reported to promote olefin aziridination under catalytic amidation conditions,[17] suggesting that a nitrene is formed during the reaction, but direct examination of such a metal−nitrenoid intermediate was again not possible.

Scheme 2. Proposed M−Nitrenoids for *Inner-Sphere* C−H Amination Reactions

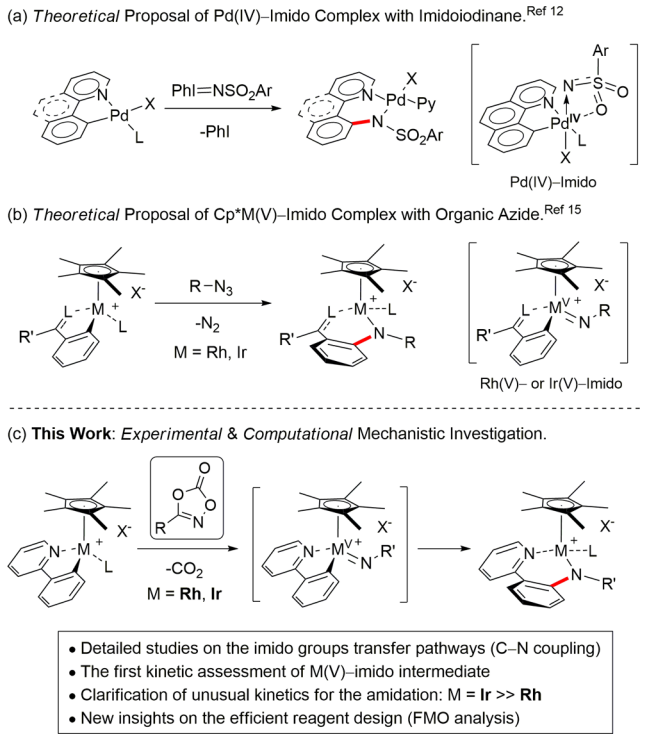

Recently, we found that the catalytic C−H amidation can be improved significantly by introducing 1,4,2-dioxazole derivatives as a novel class of aminating agents.[18] Compared to organic azides, the 1,4,2-dioxazoles allow for much milder reaction conditions, and they are easier to handle owing to increased thermal stability. During the course of our mechanistic investigation, we realized that the origin of the increased efficiency lies in much faster C−N formation. We found that the dioxazoles give amido transfer reactions that are both thermodynamically and kinetically more favorable. Motivated by these observations, we envisioned that the kinetics with 1,4,2-dioxazol-5-one may provide valuable information on the mechanism of the C−N bond forming step.

Described herein is a fully integrated experimental and computational study aimed at quantitatively assessing whether the stepwise formation of a metal−nitrenoid complex, as described in Scheme 2c, is plausible. Surprising differences in the amidation kinetics proved to be present between with Rh- and Ir-based organometallic complexes. This work constitutes the first in-depth study that explains both quantitatively and qualitatively how and why iridium is so much more competent in promoting C−N bond coupling. This new level of insight was possible because we were able to make a stoichiometric amidation model of the catalytic reaction exploiting the unique features of the new amidating agent, which was not found previously with traditional nitrogen sources, such as organic azides. Moreover, frontier orbital analyses provided fundamental general insights for the design of efficient group-transfer agents when the oxidation of metal center is involved in the reaction.

RESULTS AND DISCUSSIONS

Whereas organic azides were successfully used as aminating agents within the *inner-sphere* C−H amination strategy, these reactions typically require variable reaction temperatures making them less desirable in synthesis. The thermally unstable nature of the azides requires special caution during preparation and handling of these reagents. We recently found that 1,4,2-dioxazole derivatives[19] can serve as efficient N-sources in the Cp*Rh(III)-catalyzed C−H amidation reaction, as highlighted in eq 1.[18a] Importantly, the aforementioned problems

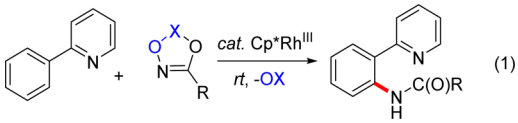

associated with the organic azides can be avoided by using dioxazoles as the amino precursors. Because dioxazoles react under much milder conditions than organic azides, they offer a more efficient and safer route to nitrogen-containing molecules. The potential relevance of this new methodology in large scale production regarding safety, sustainability, and scalability was demonstrated by successfully carrying out a decagram-scale reaction.[18b] Additional studies by Li,[20] Jiao,[21] Ackermann,[22] Glorius,[23] and others[24] proved that these novel amidating agents are also effective for isolobal d^6 catalytic systems containing Ir(III), Co(III), and Ru(II) likely following similar mechanistic reaction pathways.

DOI: 10.1021/jacs.6b08211
J. Am. Chem. Soc. 2016, 138, 14020−14029

Elementary steps of the catalytic C−H amidation under this system are illustrated in Scheme 3. The metalation of a

Scheme 3. Mechanism of Cp*Rh(III)-Catalyzed C−H Amidation

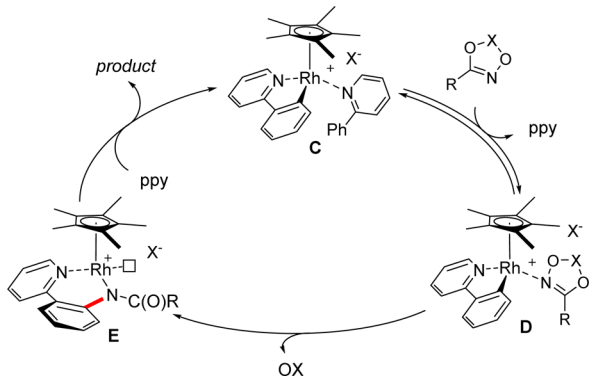

substrate, 2-phenylpyridine (ppy) as a model, via C−H activation gives the rhodacycle **C** at the formally Rh(III)-d^6 center in the pseudo-octahedral ligand environment provided by the Cp* and ppy ligands. The coordinating ppy ligand can be exchanged by the aminating reagent dioxazole to give an intermediate complex **D**. As will be explained in greater detail below, both complexes **C** and **D** coexist in equilibrium within the reaction mixture. Intermediate **D** may undergo C−N coupling accompanied by extrusion of the leaving group. The resulting Rh−amido complex **E** may subsequently react with another substrate via a concerted-metalation deprotonation (CMD) mechanism to regenerate complex **C** affording the desired product. A few acyl nitrene precursors were examined as alternative amidating agents, and 1,4,2-dioxazol-5-ones were identified as being particularly reactive, leading to room temperature reactions.

Despite identification of these elementary steps of the catalytic cycle, the key C−N bond forming process remains poorly understood. The proposed mechanism of the amido transfer is depicted in Scheme 4. Coordination of the

Scheme 4. Putative Reaction Pathways for C−N Formation

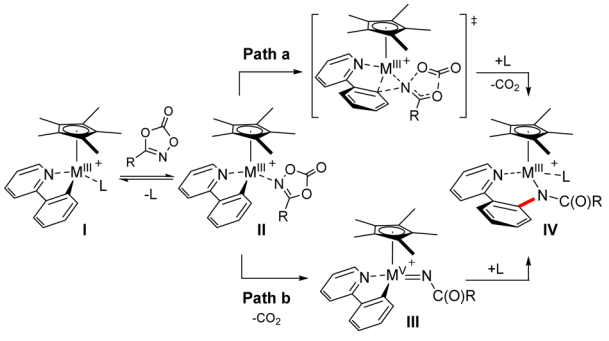

dioxazolone affords the N-bound, pseudo-octahedral 18-electron complex **II**, from which the C−N bond can be formed in two fundamentally different ways: Path a invokes a concerted S_N2-type attack of the metal−carbon bond and synchronous cleavage of CO_2. In this case, the formal oxidation state of the metal remains unchanged throughout the reaction. On the other hand, in Path b the metal−nitrogen multiple bond is formed in a stepwise fashion, to give M(V)−imido species **III**. Subsequent migratory insertion of the imido group into metal−carbon bond produces the C−N coupled product, the amido complex **IV**. The Rh(V)−imido intermediate was suggested by previous computational studies using tosyl azide as the amidating agent,[15b] but these findings have not been corroborated by experiments. Attempts at isolating the M−nitrenoid intermediate have thus far not been successful, and we were also unable to obtain spectroscopic evidence that would either support or disprove the computationally identified mechanistic proposal. In part, this lack of experimental support is due to the highly reactive nature of the key intermediates that continue to evade detection. In lieu of direct evidence within the catalytic reaction, the stoichiometric conversion of metallacyclic intermediates toward analogous nitrene precursors may be useful.[12b,13a,17,25] We sought to design a model system[26] that may capture the key component of the catalytic C−H amidation. Cyclometalated Cp*Rh(III)- and Cp*Ir(III)-complexes with the 2-phenylpyridine substrate (**1-Rh** and **1-Ir** in Scheme 5) were chosen as model systems, since both

Scheme 5. Stoichiometric Ligand Exchange with 2a

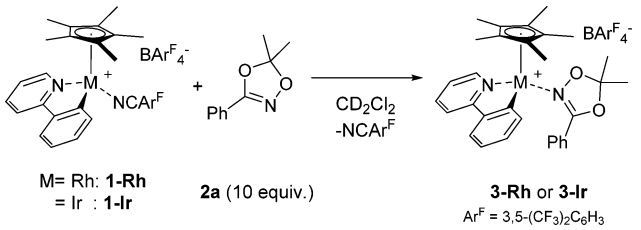

systems are found to enable C−N bond formation in a reaction with 1,4,2-dioxazole derivatives in our preliminary study. A benzonitrile carrying 3,5-bis(trifluoromethyl) substituents (Ar^FCN) was used as an innocent ligand to block an empty coordination site for mimicking the catalytic process in this stoichiometric reaction.[18a]

Comparison of the Mechanisms. We sought to compare the mechanisms promoted by the rhodium and iridium complexes by carefully constructing the energy landscapes of the stoichiometric C−N coupling reactions using density functional theory, as shown in Figure 1.[27] Not surprisingly, both metals display similar reactivity patterns in general, but significant and surprising differences are also found. Before the metal can mediate the amidation reaction, the precoordinated benzonitrile ligand Ar^FCN must be exchanged with the amidating agent, as illustrated in Scheme 4. In principle, such ligand exchange may occur following an associative or a dissociative mechanism. It is difficult to predict a priori which displacement pathway will be followed because late transition metal complexes bearing Cp* ligands are known to engage both in associative and dissociative ligand exchange mechanisms.[28]

Our computer models revealed that the dissociative pathway is much preferred, and we were unable to locate any reasonable intermediate with either of the metals carrying both the nitrile and the dioxazole ligands that would be expected in an associative process. The calculations showed that the nitrile ligand can dissociate in a unimolecular fashion with a solution phase free energy barrier of 12.8 and 15.5 kcal/mol, respectively, for Rh and Ir. As will be discussed below, this seemingly simple step becomes mechanistically important for

DOI: 10.1021/jacs.6b08211
J. Am. Chem. Soc. 2016, 138, 14020−14029

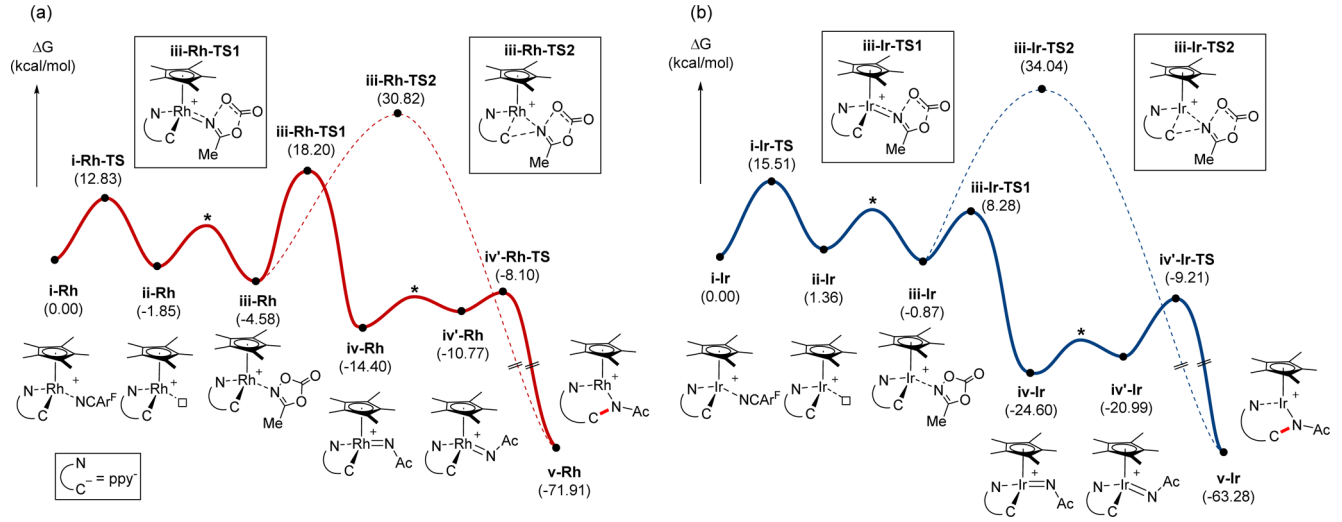

Figure 1. DFT-calculated reaction energy profiles for (a) rhodium and (b) iridium.[27] Transition states marked * were not located.

the iridium-mediated reaction and, therefore, we chose to interrogate it in greater detail.

To investigate this initial step without interference by the subsequent steps of the C−N coupling reaction, 5,5-dimethyl-3-phenyl-1,4,2-dioxazole (**2a**) was chosen as the amidating agent as summarized in Scheme 5. Compound **2a** is particularly well-suited for this purpose, as it is capable of acting as an amidating agent, but requires an elevated reaction temperature for the amidation. It allows for observing how it binds to the metal without the reaction progressing toward C−N bond formation, if we keep the reaction temperature low.[18a] The higher activation temperature is needed because the chemical driving force is lower when **2a** is used: instead of CO_2, acetone is liberated during the amido formation. When metallacycles **1-Rh** and **1-Ir** were exposed to **2a**, the nitrile ligand Ar^FCN was liberated, and the metal−dioxazole adducts **3-Rh** or **3-Ir** were formed.

A single crystal of **3-Ir** was obtained by slow diffusion of petroleum ether into a saturated dichloromethane solution at −20 °C, and the composition of **3-Ir** was unambiguously determined by X-ray diffraction studies. The fact that we are able to isolate these key intermediates is a testament of an additional benefit of the dioxazole system. Previously, it was difficult to isolate the analogous intermediates when other aminating agents, such as organic azides, were utilized.[15b,29] An ORTEP drawing of the structure of **3-Ir** is shown in Figure 2.

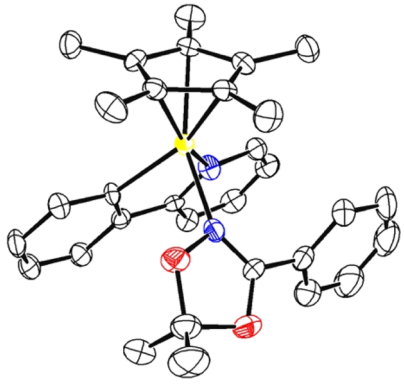

Figure 2. XRD structure of **3-Ir**. 50% probability.

The structure of the analogous rhodium complex **3-Rh** was determined in our previous work[18a] and displays very similar features as seen in **3-Ir**. The most salient bond lengths found in these two crystal structures are compared in Table 1 and Table

Table 1. Selected Bond Lengths of 3-Ir and 3-Rh[18a] in Å

	M−N(ppy)		M−N(**2a**)		M−C(ppy)	
	expt	DFT	expt	DFT	expt	DFT
3-Ir	2.090	2.127	2.095	2.141	2.080	2.057
3-Rh	2.102	2.144	2.122	2.185	2.032	2.039
Δ	−0.012	−0.017	−0.027	−0.044	0.048	0.018

S7. It was predicted that the strong relativistic contraction of the third row metal iridium gives rise to a smaller ionic radius when compared to the second row metal rhodium, which in turn affords shorter dative bonds in the iridium complex.[30] The Ir−N(ppy) and Ir−N(**2a**) bonds are 2.090 and 2.095 Å, respectively, which are 0.012 and 0.027 Å shorter than what is seen in the Rh-complex. Interestingly, the Ir−C(ppy) bond is 0.048 Å longer than the Rh−C(ppy) bond, which may be a reflection on the Rh-orbitals being closer in energy to the C-orbitals and, as a consequence, forming a more covalent, stronger, and therefore shorter Rh−C bond.

Another approach to describe the distinct interactions of Ir and Rh with ligands is using the hard/soft-acid/base (HSAB) concept: Due to the relativistic contraction of Ir, Ir(III)-complexes are expected to be much harder Lewis acids than the corresponding Rh(III) counterparts. Thus, Ir will interact more strongly with the hard nitrogen-based Lewis bases, whereas the softer carbon-based phenyl-anion ligand will prefer the softer Rh-center. These trends are reliably reproduced in our computational models, as enumerated in Table 1, confirming that these bond lengths are electronically invoked and are not based on environmental effects like crystal packing.

To determine the ligand displacement rate in the formation of dioxazole-bound metallacycles, the appearance of the ^{1}H NMR signatures of **3-Ir** or **3-Rh** was monitored below −35 °C in the presence of 10 equiv of **2a**. Reaction temperature was calibrated internally with methanol-d_4 prior to the measurement, as described in detail in the Supporting Information. The pseudo-first-order rate constants were obtained by taking the average of three independent experiments, and they showed

DOI: 10.1021/jacs.6b08211
J. Am. Chem. Soc. 2016, 138, 14020−14029

that the appearance of **3-Rh** is much faster than that of **3-Ir**, as summarized in Table S1. At −38.7 °C, the rate constant for the appearance of **3-Ir** was $4.27 \pm 0.58 \times 10^{-3}$ s^{-1}, whereas the reaction with the **3-Rh** complex was too fast to be measured reliably at this temperature. Therefore, the rate constant for the formation of **3-Rh** ($4.22 \pm 0.65 \times 10^{-3}$ s^{-1}) was determined at −50.0 °C. This finding is in excellent agreement with the DFT-calculated barriers for this process. As highlighted in Figure 1, the transition state for nitrile dissociation for **i-Rh-TS** was located at 12.8 kcal/mol, whereas 15.5 kcal/mol was found for **i-Ir-TS**. As often encountered in theoretical studies, we cannot reliably estimate the reaction rate from simple quantum chemical transition state calculations, as the pre-exponential collision factor in the Arrhenius equation cannot be obtained in this manner. However, the transition state energy difference of nearly 3 kcal/mol should translate into faster reaction for the Rh-complex, as is seen. Consistent with this mechanistic scenario is that increasing the concentration of **2a** up to 20 equiv showed no appreciable change in the rate.

All these observations suggest strongly that the ligand exchange follows a dissociative mechanism. The observation that Ir is much more reluctant to eliminate the nitrile ligand than Rh is easy to understand considering the relativistic contraction and the resulting increase in Lewis acidity that in turn leads to stronger dative bonding interactions, as mentioned above. Just as was the case in **3-Ir**, the dative bond between Ir and the nitrile ligand in **i-Ir** was stronger and shorter at 2.045 Å than in the rhodium analogue **i-Rh**, where 2.120 Å is found in our calculations.

Amidation with 1,4,2-Dioxazol-5-one. Having established a firm understanding of the ligand exchange reaction in the precursor complex, the overall amidation reactions were investigated with the most efficient amidating agent, 1,4,2-dioxazol-5-one (**2b**). Our DFT calculations summarized in Figure 1 indicate a significant difference in the abilities of the two metals in promoting an oxidative M═N coupling with concurrent extrusion of carbon dioxide, where the formal oxidation states of the Rh/Ir metal centers are changed from +III to +V. Whereas the Ir-complex **iii-Ir** is able to accomplish this step with ease traversing the transition state **iii-Ir-TS1** that lies only 9.2 kcal/mol higher in energy, the same transformation is much more difficult when rhodium is used. The energy difference between **iii-Rh** and **iii-Rh-TS1** is 22.8 kcal/mol, which is by far the highest barrier of all reaction steps and suggests that the M−nitrenoid formation accompanied by carbon dioxide extrusion may be rate-determining when Rh is used. Ir is much more reactive, and the most difficult step becomes the initial loss of the nitrile ligand with a computed barrier of 15.5 kcal/mol. Interestingly, in previous DFT studies using the aryl azides as the aminating agents, such superior reactivity of Ir compared with Rh was not found for the analogous oxidation step.[15a] Another study with tosyl azide also expected that the Ir-complex would have a marginally lower activation barrier than the Rh-complex.[16c] Once the M−nitrenoids **iv-Rh/Ir** are formed, the C−N bond coupling proceeds with little difficulty to afford the final product. These mechanistic differences are somewhat surprising and demand additional supporting evidence and ultimately an intuitive explanation. It should be noted that recent computational studies by Xia identified that similar Cp*Rh(V)−nitrenoid complexes are key intermediates catalyzing C−H functionalizations when oxidizing directing groups are employed.[16a,b] Houk and Wu also found that the pathway involving the formation of Cp*Rh(V)−nitrenoid is more kinetically favored than the non-nitrenoid pathway.[16d]

As indicated in Figure 1, we have explicitly considered an alternative reaction pathway. After association of dioxazolone to form intermediate **iii-Rh** or **iii-Ir**, the C−N bond may be formed following an S_N2-type mechanism, as outlined in Scheme 4 as Path a. The transition state for the formation of the C−N bond and synchronous cleavage of CO_2 was found to be much higher at 30.8 kcal/mol (**iii-Rh-TS2**) or 34.0 kcal/mol (**iii-Ir-TS2**) than the asynchronous pathway described above. Thus, this alternative mechanism can be excluded from further considerations.

In search of corroborating evidence for the proposal that the rate-limiting steps are different depending on the metal used, we carried out a series of experiments: 1,4,2-dioxazol-5-one (**2b**) was added to a chilled solution of **1-Rh** or **1-Ir**, which converted both complexes quantitatively to the corresponding metal−amido complexes **4-Rh** and **4-Ir** with the extrusion of stoichiometric amounts of carbon dioxide, as illustrated in Scheme 6. The formations of metal−amido complexes were

Scheme 6. Stoichiometric Amidation with 2b

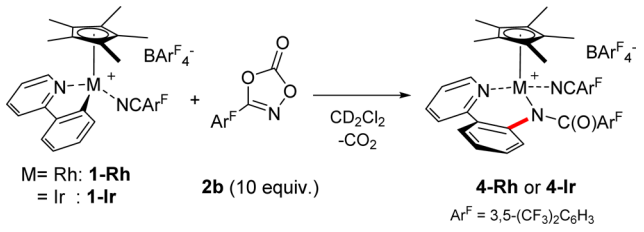

confirmed using NMR techniques by comparison with reported spectra,[26e,31] and the concentrations of the reactants and products were monitored, as shown in Figure 3.

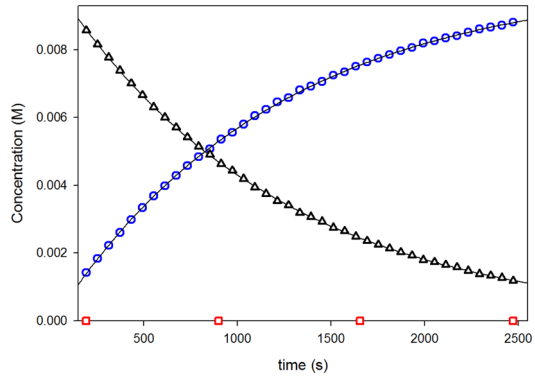

Figure 3. Amidation profile at −47.7 °C: black triangle, [**1-Ir**]; blue circle, [**4-Ir**]; red square, [**4-Rh**]. Data were fit (R^2 = 0.999) to first-order exponential decay.

In the presence of 10 equiv of **2b**, the reactions showed pseudo-first-order kinetics behavior over a time period corresponding to at least 3 times the estimated half-lifetime of the reactant species. Interestingly, the reaction rates were dramatically different for the two metal systems. At −47.7 °C, the first-order decay constant of **1-Ir** to **4-Ir** was determined to be 8.63×10^{-4} s^{-1} (black triangle and blue circle in Figure 3), whereas no formation was observable for **4-Rh** within a reaction time window of 3 h (red square in Figure 3). Only when the temperature was raised significantly were we able to

DOI: 10.1021/jacs.6b08211
J. Am. Chem. Soc. 2016, 138, 14020−14029

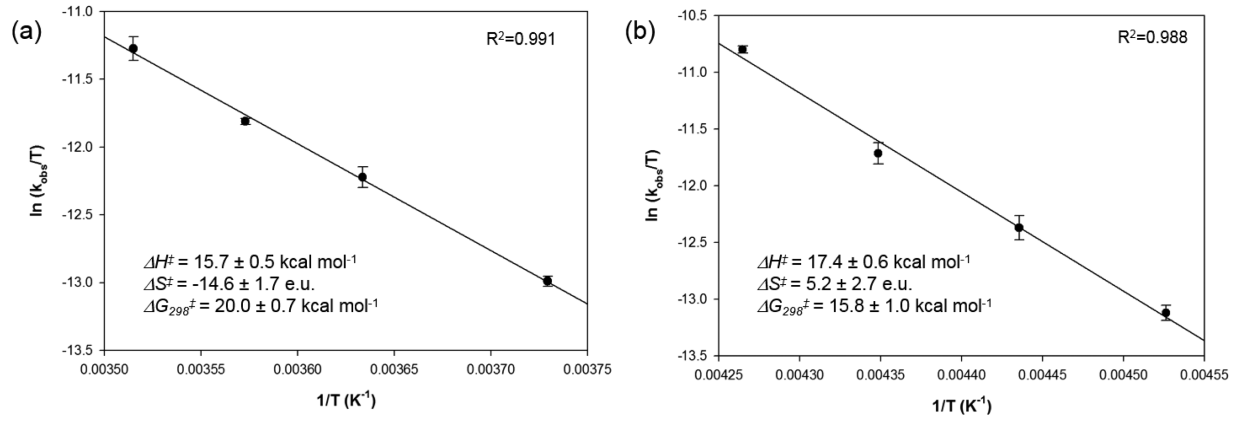

Figure 4. Eyring plots for (a) rhodium and (b) iridium.

detect the amidation product, and at 6.7 °C the rate constant was measured to be 2.08×10^{-3} s^{-1}.

To extract the enthalpy and entropy components of the free energy of activation, the rate of the reaction was obtained in variable temperature experiments, and the results were used to construct the Eyring plots, shown in Figure 4. Linear regressions gave excellent correlation in both cases, and we were able to extract the activation free energies at 298.15 K ($\Delta G_{298}^{\ddagger}$) to be 20.0 and 15.8 kcal/mol for **1-Rh** and **1-Ir**, respectively, as shown in Table 2. These experimental numbers

Table 2. Summary of Activation Parameters

	k (s^{-1}) 6.7 °C	$\Delta H^{\ddagger}$ (kcal mol^{-1})	$\Delta S^{\ddagger}$ (e.u.)	$\Delta G_{298}^{\ddagger}$ (kcal mol^{-1})
Rh	2.08×10^{-3}	15.7 ± 0.5	−14.6 ± 1.7	20.0 ± 0.7
Ir	2.2[a]	17.4 ± 0.6	5.2 ± 2.7	15.8 ± 1.0

[a]The value was extrapolated from an Eyring plot.

are in good agreement with the computed values of 22.8 and 15.5 kcal/mol, mentioned above. The decay constants provide a clear comparison between the Rh- and Ir-based amidation reactions: as shown in Table 2 and Table S5, the iridium complex at −47.7 and 6.7 °C was ∼400 and ∼1100 times faster in producing the C−N coupled product than rhodium, respectively. The good agreements of the barriers between these experimental findings and our DFT-calculated results were encouraging, but we sought to find additional support for the conclusion that the nitrile ligand extrusion is rate-limiting in the Ir-mediated reaction, while the formation of a metal−imido species by releasing CO_2 is most difficult when Rh is used for the same reaction. It is noteworthy that the S_N2-type mechanism via **iii-Rh-TS2** or **iii-Ir-TS2** is not in accord with the experimentally determined activation parameters and does not reproduce the superior reactivity of iridium in the amidation.

Inspecting the components of the activation free energies in greater detail, we note that the signs of the activation entropies ($\Delta S^{\ddagger}$) are different. In the case of the iridium complex, we found a $\Delta S^{\ddagger}$ of +5.2 e.u., but in the case of rhodium the entropy of activation is −14.6 e.u., indicating that the nature of the rate-limiting transition state is fundamentally different, consistent with what we concluded on the basis of our DFT calculations. The magnitude of the experimentally determined entropies of activation suggests that only very little free particle character is present at the respective transition states. The cleavage of the Ir−$NCAr^F$ bond is a simple bond dissociation event with very little electronic rearrangement, and thus, it is plausible that the entropy of activation, + 5.2 e.u., is slightly positive due to some of the translational entropy gain materializing at the transition state, while the Ir−$NCAr^F$ bond is weakened. The carbon dioxide release step is accompanied by a significantly more pronounced electronic reorganization. Concomitant to the carbon dioxide being released, the Rh-center is oxidized, and the Rh−nitrenoid double bond is formed formally, which leads to a much stronger Lewis acidic Rh(V)-center. This increase in formal

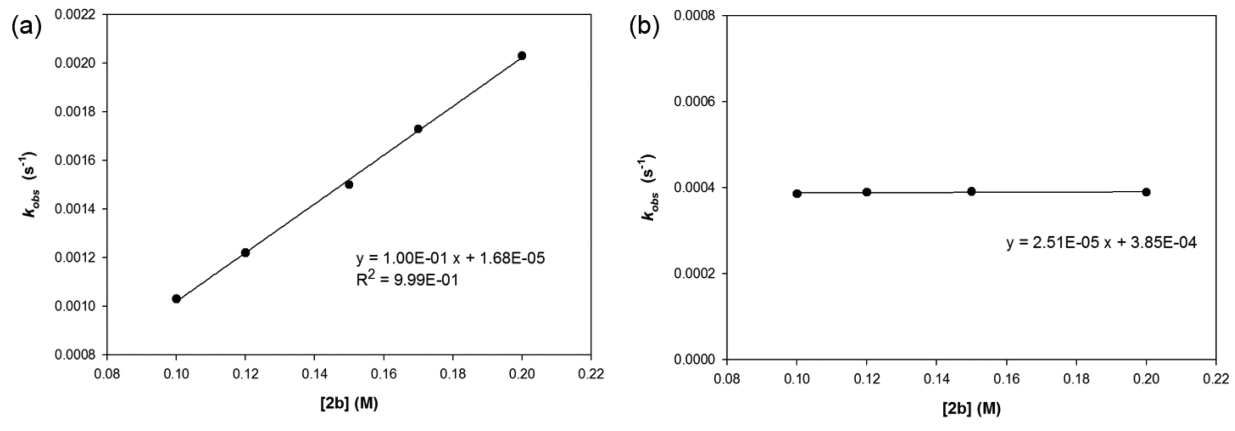

Figure 5. Reaction rate constants for (a) rhodium and (b) iridium as a function of [**2b**].

DOI: 10.1021/jacs.6b08211
J. Am. Chem. Soc. 2016, 138, 14020−14029

oxidation state will naturally lead to stronger interactions of the metal center with all ligands present in the molecule, which in turn will decrease the number of accessible, low-energy vibronic quantum states, as they shift to higher energies. Such a reduction of accessible vibrational microstates is expected to lead to a decrease in the entropy. Thus, the experimentally observed entropy of activation of −14.6 e.u. for the Rh-system is fully consistent with the transition state being that of Rh−nitrenoid formation.

Upon careful examination of the reaction rates at various temperatures, it is interesting that the amidation rate of **1-Ir** with **2b** was essentially identical with the nitrile ligand exchange rate with **2a**. As listed in Tables S1 and S2, the rate constant discrepancy for the formation of **3-Ir** ($4.27 \pm 0.58 \times 10^{-3}$ s^{-1}) and **4-Ir** ($4.79 \pm 0.15 \times 10^{-3}$ s^{-1}) at −38.7 °C is within experimental error range. Nearly the same rates between two different but related reactions substantiate the DFT-based proposal that the nitrile dissociation is the rate-limiting step for Ir-mediated amidation.

To further support the mechanistic assignment that the dioxazolone is intimately involved in the rate-limiting step in the Rh-system, but not at all important for the rate-limiting step in the Ir-system, we repeated the amidation experiments with varying amounts of the dioxazolone substrate in the reaction mixture.[27] If the transition state for the Rh−nitrenoid formation is involved in the rate-limiting step, the pseudo-first-order rate constant should be proportional to the concentration of dioxazolone.[15b] If the dissociation of the nitrile ligand is the rate-determining step, as we propose for the Ir-system, the reaction rate should not be affected by the amount of dioxazolone in solution. As shown in Figure 5a, a clear first-order dependence was observed for the rhodium complex as a function of [**2b**] in the range 10−20 equiv. For the iridium complex, the same experiment shows that the rate of the reaction is independent of the concentration of **2b** within the same concentration range, as illustrated in Figure 5b.

Molecular Orbital Analysis. From a fundamental perspective, the difference in mechanism discussed above stems from the fact that Ir is much more reactive toward oxidative Ir−nitrenoid formation, leading to facile C−N bond coupling. The barrier is so low that the otherwise relatively innocent elimination of the placeholder ligand, Ar^FCN, at the initiation step has become rate-determining. To better understand the electronic foundation for this behavior, we examined the frontier molecular orbitals (FMOs) of the molecular species involved in the oxidative M−N coupling, namely, **iii-M**, **iii-M-TS1**, and **iv-M**. Qualitatively, the changes in the FMOs during the M−imido formation are identical for both metals, as summarized conceptually in Figure 6. As the carbon dioxide fragment is expelled, a vacant p_z orbital is generated on the N-fragment of the dioxazolone, which is used to carry out the oxidative M−N coupling with the M(III)-center. Detailed discussion on the electronic reorganization is placed in the Supporting Information.

Upon inspection of the reaction energy profiles shown in Figure 1 in greater detail, the relative energy differences between the Ir- and Rh-complexes at corresponding stages of the reaction are interesting: compared to the initial reactant complex **i-M**, the dioxazolone-bound intermediate **iii-Rh** is more stable at −4.6 kcal/mol than its iridium analogue **iii-Ir**, which registered a relative solution free energy of only −0.9 kcal/mol. The CO_2 eliminating transition state **iii-Ir-TS1** was found at a relative energy of 8.3 kcal/mol that is nearly 10 kcal/mol lower than **iii-Rh-TS1**, which is found to be 18.2 kcal/mol. Interestingly, the Ir−imido complex **iv-Ir** was found at −24.6 kcal/mol and also about 10 kcal/mol lower in energy than **iv-Rh**, which has a relative energy of only −14.4 kcal/mol.

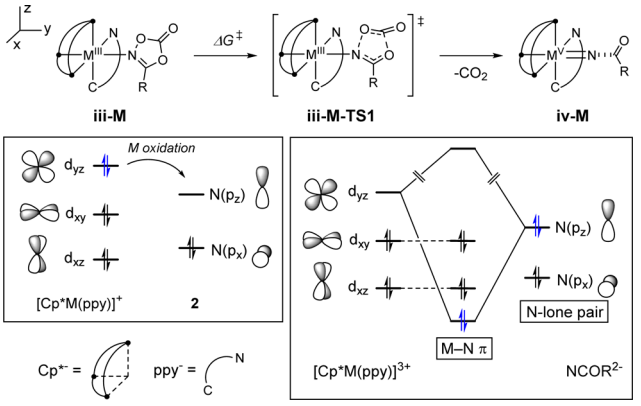

Figure 6. Conceptual MO-diagram showing the electronic structure change for the M−nitrenoid formation.

These almost identical energy differences of the transition states and M−imido intermediates are of course not coincidental and indicate that the transition states are "late" with respect to their electronic structure distortions. In other words, at the transition state, the electronic reorganization that gives rise to the energetic difference between the two intermediates has already developed fully. Indeed, the energy decomposition analysis of the complexes **iii-M**, **iii-M-TS1**, and **iv-M** clearly supports the idea that the free energy differences are the results of the electronic interactions between the $[Cp^*M(ppy)]^{n+}$ fragment and the N source moiety, as described in Supporting Information. Significantly shortened distances of the M−N(dioxazolone) bond in the transition states strongly suggest that changes in orbital interactions between M(d_{yz}) and N(p_z) have already matured: Ir−N bond lengths of **iii-Ir**, **iii-Ir-TS1**, and **iv-Ir** are 2.136, 1.867, and 1.857 Å, respectively, as shown in Figure 7 and Supporting Information. It is for this reason that the relative thermodynamic stabilities of M−imidos are transposed onto the transition states. It is important to note that dioxazolone is unique in facilitating such a "late" transition state because the N−O and C−O bonds are being broken in a concerted fashion, as there is no intermediate. However, the process is asynchronous, as the N−O bond is cleaved early and is almost broken at the transition state, while the C−O bond remains intact, as shown in Figure 7. The C−O bond breaking takes place after the transition state is traversed. Bond lengths of N−O and C−O bonds in the transition state are 2.244 and 1.612

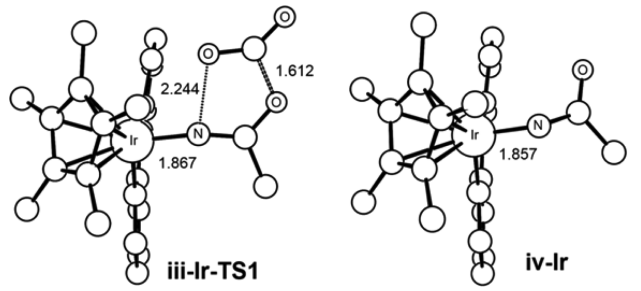

Figure 7. DFT-optimized structures of **iii-Ir-TS1** and **iv-Ir**.

DOI: 10.1021/jacs.6b08211
J. Am. Chem. Soc. 2016, 138, 14020−14029

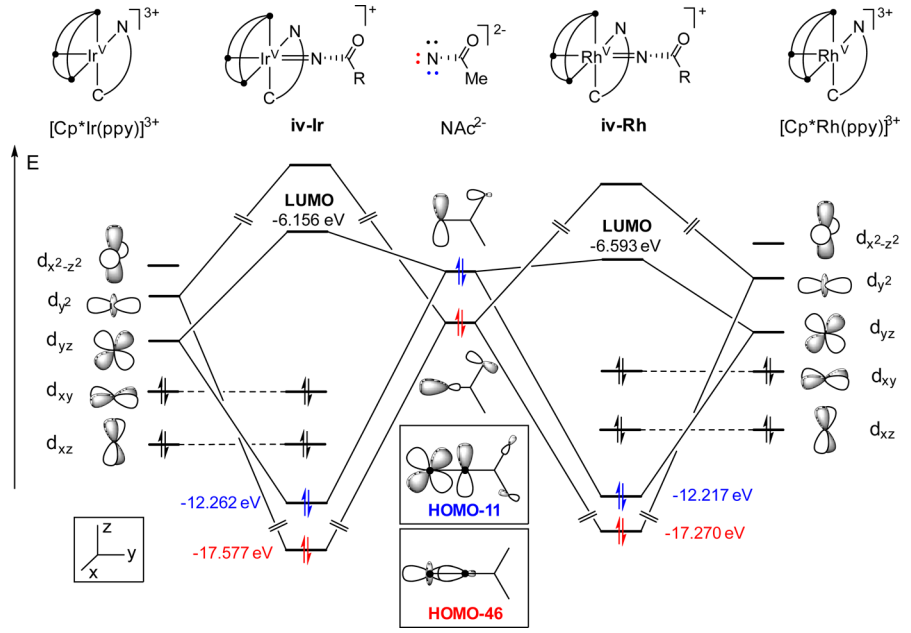

Figure 8. Quantitative MO-diagram comparing the Ir−imido (**iv-Ir**) to the Rh−imido (**iv-Rh**) bond.

Å, respectively, and elongated N−O distance facilitates the orbital overlap with N(p_z) and M(d_{yz}) being maximized. It is interesting to compare this mode of action with that of N_2 cleavage of organic azides, as described in previous studies.[15a,16c] Since N_2 dissociation is a one-bond cleaving event, it is difficult to fully develop an empty N(p_z) orbital at the transition state, and the interaction between the metal and the azide moiety is necessarily weaker. Therefore, the nature of N_2-cleaving transition state is largely unperturbed by the stability of the M−imido species, and it can be further generalized that the N_2-cleaving transition state should be higher in energy than the CO_2-cleaving analogues. Whereas the structural differences between the organic azides and the dioxazolones are obvious, its consequence on the electronics of the C−N coupling is impossible to predict without the precise analysis of the DFT calculations presented here.

This qualitative FMO analysis highlights that the key to understanding the kinetics of imido forming step lies in delineating the relative energies of the intermediates **iv-Rh** versus **iv-Ir**. Figure 8 shows an MO-diagram that compares the frontier orbitals of the two complexes, **iv-Rh** and **iv-Ir**. As mentioned above, the fragment orbitals of the iridium center are smaller in spatial extension and lower in energy, thus making the Ir(V)-center a harder Lewis acid than the Rh(V)-analogue. This electronic structure is reflected in lower-energy fragment orbitals, as indicated in Figure 8 for the M-fragments. Note that this energy ordering is classically not expected, since the Ir-orbitals carry a higher main quantum number than the Rh-orbitals, and are the results of the more pronounced relativistic contraction of Ir. Consequently, the Ir−N σ-bonding orbital was found at −17.577 eV, which is nearly 0.3 eV lower than the corresponding orbital that promotes the Rh−N σ-bonding interaction at −17.270 eV. Similarly, the M−N π-bond is formed between the p_z-lone-pair orbital of the imido ligand and the metal-d(yz) orbitals of the metal centers, as discussed above and marked in blue in Figure 8. In the Ir−imido fragment, this frontier orbital was found at −12.262 eV, whereas the same MO was located at −12.217 eV in the **iv-Rh**. These energy differences in the M−N bonding manifold are a direct illustration of the HSAB principle and provide an intuitively understandable rationale for the energetics that we found in our computational studies. At the transition state, the same interactions exist and give rise ultimately to the observed efficiency in M=N bond formation. The calculated Ir−N π and π^* orbitals are shown in Figure 9.

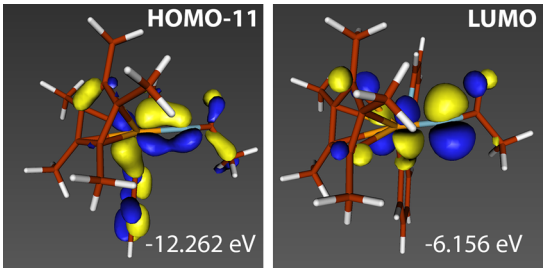

Figure 9. Kohn−Sham orbital plots (isodensity value: 0.05 au) of π and π^* orbitals of **iv-Ir**.

CONCLUSIONS

Combining computational reaction modeling with experimental techniques of mechanistic inquiry, we were able to establish a solid mechanistic understanding of how Rh(III)- and Ir(III)-centers are able to promote oxidative M−N coupling to afford a M(V)−imido complex, which can subsequently undergo C−N bond forming reactions. These studies were carried out as stoichiometric models of the catalytic amination reactions and reveal new insights that are highly relevant for the C−H functionalization.

We quantified the rates of the initial ligand dissociation and the amidation, which allowed for studying each of the catalytic steps in an isolated manner. The observed higher reactivity of the Ir-complex in the amidation was successfully rationalized by the novel bonding feature of a dioxazole-based amidating reagent and the transposition of thermodynamic stability of the Ir(V)-intermediate to the kinetic barrier. Another possible mechanism, the synchronous CO_2 extrusion and C−N

DOI: 10.1021/jacs.6b08211
J. Am. Chem. Soc. 2016, 138, 14020−14029

formation without requiring a change in oxidation state of the metal, is not found to be consistent with the experimentally determined activation parameters and does not explain the dramatically higher reactivity of iridium compared to rhodium in the amidation reaction. This work constitutes the first fully integrated experimental and theoretical study supporting the involvement of the high-valent M(V)−imido intermediates in an *inner-sphere* type of amination mechanism. In addition to evaluating reaction energies, the unique advantage of quantum chemical methods[32] lies in the frontier molecular orbital analysis that provides deep and intuitively understandable concepts of bonding that are valid and useful. In this case, the key concept that is responsible for the low barriers of the Ir-based reactions is that Ir(III) and Ir(V) are harder and stronger Lewis acids than the Rh(III) and Rh(V) analogues. The dioxazolone gives a late transition state for the oxidative coupling step that can fully take advantage of the strong M−N bonding. They are able to interact much more favorably with the N-based ligands that are strong and hard Lewis bases, which is ultimately responsible for the superior performance of the Ir catalysts for these types of reactions. We anticipate that the principles we outlined herein will be valid for many reactions of this type and this work may serve as a showcase example for the rational design of novel and efficient agents for group-transfer reactions.

■ ASSOCIATED CONTENT

Supporting Information

The Supporting Information is available free of charge on the ACS Publications website at DOI: 10.1021/jacs.6b08211.

Detailed experimental procedures, characterization of new compounds, kinetic profiles, X-ray analysis of **3-Ir**, and Cartesian coordinates of DFT-optimized structures (PDF)

Crystallographic information (CIF)

■ AUTHOR INFORMATION

Corresponding Authors

*mbaik2805@kaist.ac.kr

*sbchang@kaist.ac.kr

Notes

The authors declare no competing financial interest.

■ ACKNOWLEDGMENTS

This article is dedicated to Professor Naoto Chatani on the occasion of his 60th birthday. We thank Ms. Seohee Oh and Mr. Jin Kim (KAIST) for helpful discussions. This research was supported by the Institute for Basic Science (IBS-R010-D1) in Korea.

■ REFERENCES

(1) (a) Ricci, A. *Amino Group Chemistry: From Synthesis to the Life Sciences*; Wiley-VCH: Weinheim, 2008. (b) Candeias, N. R.; Branco, L. C.; Gois, P. M.; Afonso, C. A. M.; Trindade, A. F. *Chem. Rev.* **2009**, *109*, 2703.

(2) (a) Crabtree, R. H. *J. Chem. Soc., Dalton Trans.* **2001**, 2437. (b) Dick, A. R.; Sanford, M. S. *Tetrahedron* **2006**, *62*, 2439. (c) Collet, F.; Dodd, R. H.; Dauban, P. *Chem. Commun.* **2009**, 5061.

(3) Selected examples on the synthesis of metal−imido complexes: (a) Harlan, E. W.; Holm, R. H. *J. Am. Chem. Soc.* **1990**, *112*, 186. (b) Glueck, D. S.; Wu, J.; Hollander, F. J.; Bergman, R. G. *J. Am. Chem. Soc.* **1991**, *113*, 2041. (c) Perez, P. J.; White, P. S.; Brookhart, M.; Templeton, J. L. *Inorg. Chem.* **1994**, *33*, 6050. (d) Au, S.-M.; Fung, W.-H.; Huang, J.-S.; Cheung, K.-K.; Che, C.-M. *Inorg. Chem.* **1998**, *37*, 6564. (e) Dai, X.; Kapoor, P.; Warren, T. H. *J. Am. Chem. Soc.* **2004**, *126*, 4798. (f) Kogut, E.; Wiencko, H. L.; Zhang, L.; Cordeau, D. E.; Warren, T. H. *J. Am. Chem. Soc.* **2005**, *127*, 11248. (g) Ni, C.; Fettinger, J. C.; Long, G. J.; Brynda, M.; Power, P. P. *Chem. Commun.* **2008**, 6045. (h) Moret, M.-E.; Peters, J. C. *Angew. Chem., Int. Ed.* **2011**, *50*, 2063. (i) Wiese, S.; McAfee, J. L.; Pahls, D. R.; McMullin, C. L.; Cundari, T. R.; Warren, T. H. *J. Am. Chem. Soc.* **2012**, *134*, 10114. (j) Spasyuk, D. M.; Carpenter, S. H.; Kefalidis, C. E.; Piers, W. E.; Neidig, M. L.; Maron, L. *Chem. Sci.* **2016**, *7*, 5939.

(4) Selected reviews on the outer-sphere C−H amination: (a) Lu, H.; Zhang, X. P. *Chem. Soc. Rev.* **2011**, *40*, 1899. (b) Stokes, B. J.; Driver, T. G. *Eur. J. Org. Chem.* **2011**, *2011*, 4071. (c) Ramirez, T. A.; Zhao, B.; Shi, Y. *Chem. Soc. Rev.* **2012**, *41*, 931. (d) Jeffrey, J. L.; Sarpong, R. *Chem. Sci.* **2013**, *4*, 4092. (e) Uchida, T.; Katsuki, T. *Chem. Rec.* **2014**, *14*, 117. (f) Du Bois, J. *Org. Process Res. Dev.* **2011**, *15*, 758. (g) Schafer, A. G.; Blakey, S. B. *Chem. Soc. Rev.* **2015**, *44*, 5969. (h) Jana, N.; Driver, T. G. *Org. Biomol. Chem.* **2015**, *13*, 9720.

(5) (a) Au, S.-M.; Huang, J.-S.; Yu, W.-Y.; Fung, W.-H.; Che, C.-M. *J. Am. Chem. Soc.* **1999**, *121*, 9120. (b) Liang, J.-L.; Huang, J.-S.; Yu, X.-Q.; Zhu, N.; Che, C.-M. *Chem. - Eur. J.* **2002**, *8*, 1563. (c) Leung, S. K.-Y.; Tsui, W.-M.; Huang, J.-S.; Che, C.-M.; Liang, J.-L.; Zhu, N. *J. Am. Chem. Soc.* **2005**, *127*, 16629. (d) Fantauzzi, S.; Gallo, E.; Caselli, A.; Ragaini, F.; Casati, N.; Macchi, P.; Cenini, S. *Chem. Commun.* **2009**, 3952.

(6) (a) Perry, R. H.; Cahill, T. J., III; Roizen, J. L.; Du Bois, J.; Zare, R. N. *Proc. Natl. Acad. Sci. U. S. A.* **2012**, *109*, 18295. (b) Harvey, M. E.; Musaev, D. G.; Du Bois, J. *J. Am. Chem. Soc.* **2011**, *133*, 17207. (c) Kornecki, K. P.; Berry, J. F. *Chem. - Eur. J.* **2011**, *17*, 5827. (d) Kornecki, K. P.; Berry, J. F. *Chem. Commun.* **2012**, *48*, 12097. (e) Warzecha, E.; Berto, T. C.; Berry, J. F. *Inorg. Chem.* **2015**, *54*, 8817. (f) Varela-Alvarez, A.; Yang, T.; Jennings, H.; Kornecki, K. P.; Macmillan, S. N.; Lancaster, K. M.; Mack, J. B. C.; Du Bois, J.; Berry, J. F.; Musaev, D. G. *J. Am. Chem. Soc.* **2016**, *138*, 2327.

(7) (a) King, E. R.; Hennessy, E. T.; Betley, T. A. *J. Am. Chem. Soc.* **2011**, *133*, 4917. (b) Iovan, D. A.; Betley, T. A. *J. Am. Chem. Soc.* **2016**, *138*, 1983.

(8) Bryant, J. R.; Mayer, J. M. *J. Am. Chem. Soc.* **2003**, *125*, 10351.

(9) Selected literature references on C−H functionalization: (a) Murai, S.; Kakiuchi, F.; Sekine, S.; Tanaka, Y.; Kamatani, A.; Sonoda, M.; Chatani, N. *Nature* **1993**, *366*, 529. (b) Davies, D. L.; Donald, S. M. A.; Al-Duaij, O.; Macgregor, S. A.; Pölleth, M. *J. Am. Chem. Soc.* **2006**, *128*, 4210. (c) Davies, D. L.; Donald, S. M. A.; Al-Duaij, O.; Fawcett, J.; Little, C.; Macgregor, S. A. *Organometallics* **2006**, *25*, 5976. (d) Li, L.; Brennessel, W. W.; Jones, W. D. *J. Am. Chem. Soc.* **2008**, *130*, 12414. (e) Seregin, I. V.; Gevorgyan, V. *Chem. Soc. Rev.* **2007**, *36*, 1173. (f) Colby, D. A.; Bergman, R. G.; Ellman, J. A. *Chem. Rev.* **2010**, *110*, 624. (g) Cho, S. H.; Kim, J. Y.; Kwak, J.; Chang, S. *Chem. Soc. Rev.* **2011**, *40*, 5068. (h) Li, H.; Li, B.-J.; Shi, Z.-J. *Catal. Sci. Technol.* **2011**, *1*, 191. (i) Davies, H. M. L.; Morton, D. *Chem. Soc. Rev.* **2011**, *40*, 1857. (j) Wencel-Delord, J.; Droge, T.; Liu, F.; Glorius, F. *Chem. Soc. Rev.* **2011**, *40*, 4740. (k) Ackermann, L. *Chem. Rev.* **2011**, *111*, 1315. (l) Rouquet, G.; Chatani, N. *Angew. Chem., Int. Ed.* **2013**, *52*, 11726. (m) Daugulis, O.; Roane, J.; Tran, L. D. *Acc. Chem. Res.* **2015**, *48*, 1053. (n) Gensch, T.; Hopkinson, M. N.; Glorius, F.; Wencel-Delord, J. *Chem. Soc. Rev.* **2016**, *45*, 2900. (o) He, G.; Wang, B.; Nack, W. A.; Chen, G. *Acc. Chem. Res.* **2016**, *49*, 635. (p) Davies, H. M. L.; Morton, D. *J. Org. Chem.* **2016**, *81*, 343.

(10) Selected reviews on the inner-sphere C−H amination: (a) Matsuda, N.; Hirano, K.; Satoh, T.; Miura, M. *Synthesis* **2012**, *44*, 1792. (b) Mei, T.-S.; Kou, L.; Ma, S.; Engle, K. M.; Yu, J.-Q. *Synthesis* **2012**, *44*, 1778. (c) Louillat, M.-L.; Patureau, F. W. *Chem. Soc. Rev.* **2014**, *43*, 901. (d) Jiao, J.; Murakami, K.; Itami, K. *ACS Catal.* **2016**, *6*, 610. (e) Kim, H.; Chang, S. *ACS Catal.* **2016**, *6*, 2341. (f) Subramanian, P.; Rudolf, G. C.; Kaliappan, K. P. *Chem. - Asian J.* **2016**, *11*, 168.

(11) (a) Wendlandt, A. E.; Suess, A. M.; Stahl, S. S. *Angew. Chem., Int. Ed.* **2011**, *50*, 11062. (b) Huffman, L. M.; Stahl, S. S. *J. Am. Chem. Soc.* **2008**, *130*, 9196. (c) Suess, A. M.; Ertem, M. Z.; Cramer, C. J.; Stahl,

S. S. *J. Am. Chem. Soc.* **2013**, *135*, 9797. (d) Pendleton, I. M.; Pérez-Temprano, M. H.; Sanford, M. S.; Zimmerman, P. M. *J. Am. Chem. Soc.* **2016**, *138*, 6049.
(12) (a) Thu, H.-Y.; Yu, W.-Y.; Che, C.-M. *J. Am. Chem. Soc.* **2006**, *128*, 9048. (b) Dick, A. R.; Remy, M. S.; Kampf, J. W.; Sanford, M. S. *Organometallics* **2007**, *26*, 1365. (c) Ng, K.-H.; Chan, A. S. C.; Yu, W.-Y. *J. Am. Chem. Soc.* **2010**, *132*, 12862. (d) Xiao, B.; Gong, T.-J.; Xu, J.; Liu, Z.-J.; Liu, L. *J. Am. Chem. Soc.* **2011**, *133*, 1466. (e) Ke, Z.; Cundari, T. R. *Organometallics* **2010**, *29*, 821.
(13) (a) Kim, J. Y.; Park, S. H.; Ryu, J.; Cho, S. H.; Kim, S. H.; Chang, S. *J. Am. Chem. Soc.* **2012**, *134*, 9110. (b) Ryu, J.; Kwak, J.; Shin, K.; Lee, D.; Chang, S. *J. Am. Chem. Soc.* **2013**, *135*, 12861. (c) Kang, T.; Kim, Y.; Lee, D.; Wang, Z.; Chang, S. *J. Am. Chem. Soc.* **2014**, *136*, 4141. (d) Park, S. H.; Park, Y.; Chang, S. *Org. Synth.* **2014**, *91*, 52. (e) Shin, K.; Kim, H.; Chang, S. *Acc. Chem. Res.* **2015**, *48*, 1040. (f) Kim, Y.; Park, J.; Chang, S. *Org. Lett.* **2016**, *18*, 1892.
(14) (a) Yu, D.-G.; Suri, M.; Glorius, F. *J. Am. Chem. Soc.* **2013**, *135*, 8802. (b) Zheng, Q.-Z.; Liang, Y.-F.; Qin, C.; Jiao, N. *Chem. Commun.* **2013**, *49*, 5654. (c) Pan, C.; Abdukader, A.; Han, J.; Cheng, Y.; Zhu, C. *Chem. - Eur. J.* **2014**, *20*, 3606. (d) Sun, B.; Yoshino, T.; Matsunaga, S.; Kanai, M. *Adv. Synth. Catal.* **2014**, *356*, 1491. (e) Chen, H.; Huestis, M. P. *ChemCatChem* **2015**, *7*, 743. (f) Hou, W.; Yang, Y.; Ai, W.; Wu, Y.; Wang, X.; Zhou, B.; Li, Y. *Eur. J. Org. Chem.* **2015**, *2015*, 395. (g) Pi, C.; Cui, X.; Wu, Y. *J. Org. Chem.* **2015**, *80*, 7333. (h) Ali, M. A.; Yao, X.; Li, G.; Lu, H. *Org. Lett.* **2016**, *18*, 1386. (i) Hermann, G. N.; Becker, P.; Bolm, C. *Angew. Chem., Int. Ed.* **2016**, *55*, 3781. (j) Zhang, T.; Hu, X.; Wang, Z.; Yang, T.; Sun, H.; Li, G.; Lu, H. *Chem. - Eur. J.* **2016**, *22*, 2920. (k) Zhu, B.; Cui, X.; Pi, C.; Chen, D.; Wu, Y. *Adv. Synth. Catal.* **2016**, *358*, 326.
(15) (a) Figg, T. M.; Park, S.; Park, J.; Chang, S.; Musaev, D. G. *Organometallics* **2014**, *33*, 4076. (b) Park, S. H.; Kwak, J.; Shin, K.; Ryu, J.; Park, Y.; Chang, S. *J. Am. Chem. Soc.* **2014**, *136*, 2492. (c) Ajitha, M. J.; Huang, K.-W.; Kwak, J.; Kim, H. J.; Chang, S.; Jung, Y. *Dalton Trans.* **2016**, *45*, 7980.
(16) (a) Xu, L.; Zhu, Q.; Huang, G.; Cheng, B.; Xia, Y. *J. Org. Chem.* **2012**, *77*, 3017. (b) Zhou, T.; Guo, W.; Xia, Y. *Chem. - Eur. J.* **2015**, *21*, 9209. (c) Liu, J.-B.; Sheng, X.-H.; Sun, C.-Z.; Huang, F.; Chen, D.-Z. *ACS Catal.* **2016**, *6*, 2452. (d) Yang, Y.-F.; Houk, K. N.; Wu, Y.-D. *J. Am. Chem. Soc.* **2016**, *138*, 6861.
(17) Zhang, L.-L.; Li, L.-H.; Wang, Y.-Q.; Yang, Y.-F.; Liu, X.-Y.; Liang, Y.-M. *Organometallics* **2014**, *33*, 1905.
(18) (a) Park, Y.; Park, K. T.; Kim, J. G.; Chang, S. *J. Am. Chem. Soc.* **2015**, *137*, 4534. (b) Park, Y.; Jee, S.; Kim, J. G.; Chang, S. *Org. Process Res. Dev.* **2015**, *19*, 1024. (c) Park, J.; Chang, S. *Angew. Chem., Int. Ed.* **2015**, *54*, 14103.
(19) (a) Sauer, J.; Mayer, K. K. *Tetrahedron Lett.* **1968**, *9*, 319. (b) Zhong, C. L.; Tang, B. Y.; Yin, P.; Chen, Y.; He, L. *J. Org. Chem.* **2012**, *77*, 4271. (c) Bizet, V.; Buglioni, L.; Bolm, C. *Angew. Chem., Int. Ed.* **2014**, *53*, 5639. (d) Bizet, V.; Bolm, C. *Eur. J. Org. Chem.* **2015**, *2015*, 2854.
(20) (a) Wang, H.; Tang, G.; Li, X. *Angew. Chem., Int. Ed.* **2015**, *54*, 13049. (b) Wang, F.; Wang, H.; Wang, Q.; Yu, S.; Li, X. *Org. Lett.* **2016**, *18*, 1306.
(21) Liang, Y.; Liang, Y.-F.; Tang, C.; Yuan, Y.; Jiao, N. *Chem. - Eur. J.* **2015**, *21*, 16395.
(22) (a) Mei, R.; Loup, J.; Ackermann, L. *ACS Catal.* **2016**, *6*, 793. (b) Wang, H.; Lorion, M. M.; Ackermann, L. *Angew. Chem., Int. Ed.* **2016**, *55*, 10386.
(23) Wang, X.; Lerchen, A.; Glorius, F. *Org. Lett.* **2016**, *18*, 2090.
(24) (a) Barsu, N.; Rahman, M. A.; Sen, M.; Sundararaju, B. *Chem. - Eur. J.* **2016**, *22*, 9135. (b) Wang, J.; Zha, S.; Chen, K.; Zhang, F.; Song, C.; Zhu, J. *Org. Lett.* **2016**, *18*, 2062.
(25) (a) Sau, Y.-K.; Yi, X.-Y.; Chan, K.-W.; Lai, C.-S.; Williams, I. D.; Leung, W.-H. *J. Organomet. Chem.* **2010**, *695*, 1399. (b) Turlington, C. R.; White, P. S.; Brookhart, M.; Templeton, J. L. *Organometallics* **2015**, *34*, 4810.
(26) (a) Sanford, M. S.; Love, J. A.; Grubbs, R. H. *J. Am. Chem. Soc.* **2001**, *123*, 6543. (b) Powers, D. C.; Benitez, D.; Tkatchouk, E.; Goddard, W. A.; Ritter, T. *J. Am. Chem. Soc.* **2010**, *132*, 14092. (c) Powers, D. C.; Xiao, D. Y.; Geibel, M. A. L.; Ritter, T. *J. Am. Chem. Soc.* **2010**, *132*, 14530. (d) Ball, N. D.; Gary, J. B.; Ye, Y.; Sanford, M. S. *J. Am. Chem. Soc.* **2011**, *133*, 7577. (e) Turlington, C. R.; White, P. S.; Brookhart, M.; Templeton, J. L. *J. Am. Chem. Soc.* **2014**, *136*, 3981. (f) Lotz, M. D.; Remy, M. S.; Lao, D. B.; Ariafard, A.; Yates, B. F.; Canty, A. J.; Mayer, J. M.; Sanford, M. S. *J. Am. Chem. Soc.* **2014**, *136*, 8237.
(27) See Supporting Information for details.
(28) (a) Hinderling, C.; Plattner, D. A.; Chen, P. *Angew. Chem., Int. Ed. Engl.* **1997**, *36*, 243. (b) Rerek, M. E.; Basolo, F. *J. Am. Chem. Soc.* **1984**, *106*, 5908. (c) Fan, H.-J.; Hall, M. B. *Organometallics* **2001**, *20*, 5724. (d) O'Connor, J. M.; Casey, C. P. *Chem. Rev.* **1987**, *87*, 307. (e) Janowicz, A. H.; Bryndza, H. E.; Bergman, R. G. *J. Am. Chem. Soc.* **1981**, *103*, 1516. (f) Glueck, D. S.; Bergman, R. G. *Organometallics* **1991**, *10*, 1479.
(29) (a) Tauchert, M. E.; Incarvito, C. D.; Rheingold, A. L.; Bergman, R. G.; Ellman, J. A. *J. Am. Chem. Soc.* **2012**, *134*, 1482. (b) Tsai, A. S.; Tauchert, M. E.; Bergman, R. G.; Ellman, J. A. *J. Am. Chem. Soc.* **2011**, *133*, 1248. (c) Yu, S.; Tang, G.; Li, Y.; Zhou, X.; Lan, Y.; Li, X. *Angew. Chem., Int. Ed.* **2016**, *55*, 8696.
(30) (a) Siegbahn, P. E. M. *J. Am. Chem. Soc.* **1996**, *118*, 1487. (b) Gorin, D. J.; Toste, F. D. *Nature* **2007**, *446*, 395. (c) Pyykko, P. *Chem. Rev.* **1988**, *88*, 563. (d) Leyva-Pérez, A.; Corma, A. *Angew. Chem., Int. Ed.* **2012**, *51*, 614.
(31) Turlington, C. R.; White, P. S.; Brookhart, M.; Templeton, J. L. *J. Organomet. Chem.* **2015**, *792*, 81.
(32) Selected reviews on computational organometallic catalysis: (a) Balcells, D.; Clot, E.; Eisenstein, O. *Chem. Rev.* **2010**, *110*, 749. (b) Lodewyk, M. W.; Siebert, M. R.; Tantillo, D. J. *Chem. Rev.* **2012**, *112*, 1839. (c) Sperger, T.; Sanhueza, I. A.; Kalvet, I.; Schoenebeck, F. *Chem. Rev.* **2015**, *115*, 9532. (d) Park, Y.; Ahn, S.; Kang, D.; Baik, M.-H. *Acc. Chem. Res.* **2016**, *49*, 1263. (e) Sperger, T.; Sanhueza, I. A.; Schoenebeck, F. *Acc. Chem. Res.* **2016**, *49*, 1311. (f) Guan, C. S.; Cundari, T. R. *Comput. Theor. Chem.* **2016**, *1091*, 64.

DOI: 10.1021/jacs.6b08211
J. Am. Chem. Soc. 2016, 138, 14020−14029